

PROJECTING ONTO THE UNIT DUAL QUATERNION SET

ZIYANG LI, CHUNFENG CUI, AND JIAJIN XIE

ABSTRACT. Dual quaternions have gained significant attention due to their wide applications in areas such as multi-agent formation control, 3D motion modeling, and robotics. A fundamental aspect in dual quaternion research involves the projection onto unit dual quaternion sets. In this paper, we systematically study such projections under the 2^R -norm, which is commonly used in practical applications. We identify several distinct cases based on the relationship between the standard and dual parts in vector form, and demonstrate the effectiveness of the proposed algorithm through numerical experiments.

1. INTRODUCTION

Dual quaternions, introduced by Clifford [5] in 1873, form an 8-dimensional algebra combining quaternions and dual numbers that elegantly represents 3D rigid transformations space [1, 10, 11, 21]. This mathematical framework has become indispensable across engineering fields including robotics, computer graphics, and biomechanics due to its superior handling of combined rotational and translational motions [4, 7, 8, 20]. This superiority is particularly evident in its ability to unify general screw motions with all fundamental cases of rotation and translation, such as the rotation of a robotic joint or the linear movement of a camera on a track.

Among the many research problems involving dual quaternions, projection onto the unit dual quaternion set is of fundamental importance. For instance, the hand-eye calibration problem can be formulated as a least-squares optimization of a real-valued function over dual quaternion variables, subject to a unit dual quaternion constraint [2, 12, 14, 17, 19]. When solving such problems using a proximal linearized algorithm, each iteration requires computing a projection onto the unit dual quaternion set [3, 6, 22].

In this paper, we aim to systematically investigate the projection onto the unit dual quaternion set under the 2^R -norm, a norm widely adopted in practical applications as it

Key words: unit dual quaternion, metric projection, KKT condition, linear independence constraint qualification

Mathematics subject classification (2020): 65F10, 65F20, 90C25, 15A06, 68W20

ensures that the rotational and translational components are treated with equal importance. In particular, we conduct a detailed analysis based on the first-order optimality condition (KKT condition) for constrained optimization, with particular attention to the distinct characteristics between the standard and dual parts of dual quaternions. For several special cases, we further derive closed-form expressions of the projection points. Compared with the work in [2], our analysis provides a more comprehensive and systematic treatment of the projection problem.

The rest of the paper is organized as follows. Section 2 reviews the fundamentals of quaternions and dual quaternions, then introduces the first-order optimality conditions for constrained optimization. Section 3 proposes the algorithm for projecting onto the unit dual quaternion set, which comprehensively accounts for all four possible cases. Section 4 presents numerical examples of differential standard-dual part configurations. Finally, some conclusions are drawn in Section 5.

2. PRELIMINARY

In this section, we review the definitions of quaternions, dual numbers, and dual quaternions. The sets of real numbers, quaternions, dual numbers, dual quaternions, and unit dual quaternions are denoted as \mathbb{R} , \mathbb{Q} , $\hat{\mathbb{R}}$, $\hat{\mathbb{Q}}$, and $\hat{\mathbb{U}}$ respectively.

2.1. Quaternions. A quaternion $\tilde{q} \in \mathbb{Q}$ is defined as a pair consisting of a scalar part $q_0 \in \mathbb{R}$ and a vector part $\vec{q} = (q_1, q_2, q_3)^\top \in \mathbb{R}^3$. To distinguish quaternions from real numbers, we adopt the convention of using a tilde symbol. A quaternion can then be written in either of the following equivalent forms:

$$\tilde{q} = [q_0, \vec{q}] = [q_0, q_1, q_2, q_3] = q_0 + \mathbf{i}q_1 + \mathbf{j}q_2 + \mathbf{k}q_3,$$

where $q_0, q_1, q_2, q_3 \in \mathbb{R}$, and $\mathbf{i}, \mathbf{j}, \mathbf{k}$ are the standard quaternion imaginary units, which satisfy

$$\mathbf{i}^2 = \mathbf{j}^2 = \mathbf{k}^2 = \mathbf{ijk} = -1, \quad \mathbf{ij} = -\mathbf{ji} = \mathbf{k}, \quad \mathbf{ik} = -\mathbf{ki} = \mathbf{j}, \quad \mathbf{jk} = -\mathbf{kj} = \mathbf{i}.$$

If $q_0 = 0$, then $\tilde{q} = [0, \vec{q}]$ is called a pure quaternion. The conjugate of \tilde{q} , denoted \tilde{q}^* , is defined by $\tilde{q}^* = q_0 - \mathbf{i}q_1 - \mathbf{j}q_2 - \mathbf{k}q_3$. The scalar part of \tilde{q} , denoted by $\text{Sc}(\tilde{q})$, is given by $\text{Sc}(\tilde{q}) = \frac{1}{2}(\tilde{q} + \tilde{q}^*) = q_0$. Given two quaternions $\tilde{p} = [p_0, \vec{p}]$ and $\tilde{q} = [q_0, \vec{q}]$, their sum and product are defined as follows:

$$\tilde{q} \pm \tilde{p} = [q_0 \pm p_0, \vec{q} \pm \vec{p}] \quad \text{and} \quad \tilde{q}\tilde{p} = [q_0p_0 - \vec{q} \cdot \vec{p}, p_0\vec{q} + q_0\vec{p} + \vec{q} \times \vec{p}].$$

Quaternion multiplication is associative but not commutative in general. That is, $\tilde{q}\tilde{p} \neq \tilde{p}\tilde{q}$, unless the cross product $\tilde{q} \times \tilde{p} = \vec{0}$. The magnitude (or norm) of \tilde{q} is defined as $|\tilde{q}| = \sqrt{\tilde{q}\tilde{q}^*} = \sqrt{\tilde{q}^*\tilde{q}} = \sqrt{q_0^2 + q_1^2 + q_2^2 + q_3^2}$. A quaternion \tilde{q} is called a unit quaternion if $|\tilde{q}|^2 = 1$.

2.2. Dual quaternions. Before introducing dual quaternions, we first present the concept of dual numbers. A dual number $a = a_s + a_d\epsilon \in \hat{\mathbb{R}}$ consists of a standard part $a_s \in \mathbb{R}$ and a dual part $a_d \in \mathbb{R}$. The symbol ϵ is called the infinitesimal unit, satisfying $\epsilon \neq 0$, $\epsilon^2 = 0$. If $a_s \neq 0$, then a is said to be appreciable; otherwise, it is called infinitesimal [15]. For two dual numbers $a = a_s + a_d\epsilon$ and $b = b_s + b_d\epsilon$ in $\hat{\mathbb{R}}$, their addition, multiplication, and division are defined as:

$$\begin{aligned} a + b &= a_s + b_s + (a_d + b_d)\epsilon, \\ ab &= a_s b_s + (a_s b_d + b_s a_d)\epsilon, \\ \frac{b_s + b_d\epsilon}{a_s + a_d\epsilon} &= \begin{cases} \frac{b_s}{a_s} + \left(\frac{b_d}{a_s} - \frac{b_s a_d}{a_s^2} \right) \epsilon, & \text{if } a_s \neq 0, \\ \frac{b_d}{a_d} + c\epsilon, & \text{if } a_s = 0, b_s = 0, \end{cases} \end{aligned}$$

where $c \in \mathbb{R}$ is an arbitrary real constant.

Let the set of dual quaternions be defined as

$$\hat{\mathbb{Q}} := \{\hat{q} = \tilde{q}_s + \tilde{q}_d\epsilon \mid \tilde{q}_s, \tilde{q}_d \in \mathbb{Q}\}.$$

We use a hat symbol “ $\hat{\cdot}$ ” to distinguish dual quaternions from dual numbers. In a dual quaternion $\hat{q} = \tilde{q}_s + \tilde{q}_d\epsilon$, the component \tilde{q}_s is called the standard part, and \tilde{q}_d is the dual part. Addition and subtraction of dual quaternions follow the same rules as for dual numbers. The conjugate of a dual quaternion is defined component-wise as $\hat{q}^* = \tilde{q}_s^* + \tilde{q}_d^*\epsilon$. The magnitude of \hat{q} is defined as

$$(1) \quad |\hat{q}| = \begin{cases} |\tilde{q}_s| + \frac{\text{Sc}(\tilde{q}_s^*\tilde{q}_d)}{|\tilde{q}_s|}\epsilon, & \text{if } \tilde{q}_s \neq 0, \\ |\tilde{q}_d|\epsilon, & \text{otherwise.} \end{cases}$$

A dual quaternion $\hat{q} = \tilde{q}_s + \tilde{q}_d\epsilon$ is called a unit dual quaternion if it satisfies the following two conditions:

$$(2) \quad |\tilde{q}_s| = 1 \quad \text{and} \quad \tilde{q}_s^*\tilde{q}_d + \tilde{q}_d^*\tilde{q}_s = 0.$$

For a dual quaternion $\hat{q} = \tilde{q}_s + \tilde{q}_d\epsilon \in \hat{\mathbb{Q}}$, the 2^R -norm is defined as

$$\|\hat{q}\|_{2^R} := \sqrt{|\tilde{q}_s|^2 + |\tilde{q}_d|^2}.$$

Unit dual quaternions offer a canonical and compact representation of rigid body motion. A single unit dual quaternion $\hat{q} = \tilde{q}_s + \tilde{q}_d\epsilon$, subject to the two conditions in (2), simultaneously encodes both rotation and translation. The rotation matrix $\mathbf{R} = (r_{ij}) \in \mathbb{R}^{3 \times 3}$ is represented by the unit quaternion $\tilde{q}_s = q_{s_0} + q_{s_1}\mathbf{i} + q_{s_2}\mathbf{j} + q_{s_3}\mathbf{k}$, where $q_{s_0} = \frac{1}{2}\sqrt{1 + r_{11} + r_{22} + r_{33}}$, $q_{s_1} = \frac{1}{4q_{s_0}}(r_{23} - r_{32})$, $q_{s_2} = \frac{1}{4q_{s_0}}(r_{13} - r_{31})$ and $q_{s_3} = \frac{1}{4q_{s_0}}(r_{12} - r_{21})$. When we know the unit quaternion \tilde{q}_s , we have the rotation matrix:

$$\mathbf{R} = \begin{pmatrix} q_{s_0}^2 + q_{s_1}^2 - q_{s_2}^2 - q_{s_3}^2 & 2(q_{s_1}q_{s_2} - q_{s_0}q_{s_3}) & 2(q_{s_1}q_{s_3} + q_{s_0}q_{s_2}) \\ 2(q_{s_1}q_{s_2} + q_{s_0}q_{s_3}) & q_{s_0}^2 - q_{s_1}^2 + q_{s_2}^2 - q_{s_3}^2 & 2(q_{s_2}q_{s_3} - q_{s_0}q_{s_1}) \\ 2(q_{s_1}q_{s_3} - q_{s_0}q_{s_2}) & 2(q_{s_2}q_{s_3} + q_{s_0}q_{s_1}) & q_{s_0}^2 - q_{s_1}^2 - q_{s_2}^2 + q_{s_3}^2 \end{pmatrix}.$$

The translation vector $\mathbf{t} = (t_1, t_2, t_3)^\top$ is encoded within the dual part \tilde{q}_d , and is recovered as a pure quaternion $\tilde{t} = 0 + t_1\mathbf{i} + t_2\mathbf{j} + t_3\mathbf{k}$ using the relation $\tilde{t} = 2\tilde{q}_d\tilde{q}_s^*$. One may refer to [18] for more information on the relationship between quaternions and rotations.

2.3. First-order optimality conditions. Consider the following constrained optimization problem

$$(3) \quad \min_{x \in \mathbb{R}^n} f(x) \quad \text{subject to} \quad \begin{cases} c_i(x) = 0, & i \in \mathcal{E}, \\ c_i(x) \geq 0, & i \in \mathcal{I}, \end{cases}$$

where f and the functions c_i are all smooth, real-valued functions on a subset of \mathbb{R}^n , and \mathcal{I} and \mathcal{E} are two finite sets of indices. We call f the objective function, while $c_i(x) = 0$, $i \in \mathcal{E}$ are the equality constraints and $c_i(x) \geq 0$, $i \in \mathcal{I}$ are the inequality constraints.

Definition 2.1 (Active set). The active set $\mathcal{A}(x)$ at any feasible x consists of the equality constraint indices from \mathcal{E} together with the indices of the inequality constraints i for which $c_i(x) = 0$, that is,

$$\mathcal{A}(x) = \mathcal{E} \cup \{i \in \mathcal{I} | c_i(x) = 0\}.$$

Definition 2.2 (LICQ). Given the point x and the active set $\mathcal{A}(x)$, we say that the linear independence constraint qualification (LICQ) holds if the set of active constraint gradients $\{\nabla c_i(x), i \in \mathcal{A}(x)\}$ is linearly independent.

Associated with each constraint $c_i(x)$ in (3), we introduce a Lagrange multiplier $\lambda_i \in \mathbb{R}$. Then we define the Lagrangian function for the general problem (3) as

$$\mathcal{L}(x, \lambda) = f(x) - \sum_{i \in \mathcal{E} \cup \mathcal{I}} \lambda_i c_i(x),$$

where λ is the vector of multipliers λ_i .

Theorem 2.3 (First-order necessary conditions). Suppose that $x^\# \in \mathbb{R}^n$ is a local solution of (3), the functions f and c_i in (3) are continuously differentiable, and the LICQ holds at $x^\#$. Then there is a Lagrange multiplier vector $\lambda^\# \in \mathbb{R}^{|\mathcal{E}|+|\mathcal{I}|}$, with components $\lambda_i^\#$, $i \in \mathcal{E} \cup \mathcal{I}$, such that the following conditions are satisfied at $(x^\#, \lambda^\#)$

$$\begin{aligned}\nabla_x \mathcal{L}(x^\#, \lambda^\#) &= 0, \\ c_i(x^\#) &= 0, \quad \text{for all } i \in \mathcal{E}, \\ c_i(x^\#) &\geq 0, \quad \text{for all } i \in \mathcal{I}, \\ \lambda_i^\# &\geq 0, \quad \text{for all } i \in \mathcal{I}, \\ \lambda_i^\# c_i(x^\#) &= 0, \quad \text{for all } i \in \mathcal{I}.\end{aligned}$$

The conditions above are widely known as the *Karush-Kuhn-Tucker conditions*, or *KKT conditions* for short [13].

3. PROJECT ONTO THE UNIT DUAL QUATERNION SET

3.1. Problem setup. Suppose we have a dual quaternion \hat{a} . Its projection onto the unit dual quaternion set under the 2^R -norm can be formulated as the following optimization problem:

$$(4) \quad \min_{\hat{q}} \frac{1}{2} \|\hat{q} - \hat{a}\|_{2^R}^2 \quad \text{subject to} \quad |\hat{q}| = 1.$$

To proceed, we introduce the real vector representation of dual quaternions and reformulate problem (4) into a non-convex optimization problem. To distinguish between scalars and vectors, we adopt the convention that plain symbols such as 0 denote scalars, while arrows denote vectors. For example, $\vec{0} = (0, 0, 0, 0)^\top$ denotes a four-dimensional zero vector.

A dual quaternion $\hat{q} = \tilde{q}_s + \tilde{q}_d\epsilon$ can be represented in real vector form as $\vec{\hat{q}}$, namely

$$\vec{\hat{q}} = \begin{pmatrix} \vec{\tilde{q}}_s \\ \vec{\tilde{q}}_d \end{pmatrix} = (q_{s0}, q_{s1}, q_{s2}, q_{s3}, q_{d0}, q_{d1}, q_{d2}, q_{d3})^\top, \quad \vec{\hat{q}} \in \mathbb{R}^8, \quad \vec{\tilde{q}}_s, \vec{\tilde{q}}_d \in \mathbb{R}^4,$$

where $\vec{\tilde{q}}_s = (q_{s0}, q_{s1}, q_{s2}, q_{s3})^\top$ and $\vec{\tilde{q}}_d = (q_{d0}, q_{d1}, q_{d2}, q_{d3})^\top$ denote the vectorized real and dual parts of \hat{q} , respectively. Thus, $\vec{\hat{q}}$ can be viewed as an element in an eight-dimensional real vector space spanned by the standard basis $(1, \mathbf{i}, \mathbf{j}, \mathbf{k}, \epsilon, \epsilon\mathbf{i}, \epsilon\mathbf{j}, \epsilon\mathbf{k})$. Using this representation, we now translate the unit dual quaternion constraint $|\hat{q}| = 1$ into constraints on $\vec{\tilde{q}}_s$

and $\vec{\tilde{q}}_d$. From the unit dual quaternion condition (2), it is known that

$$\left\| \vec{\tilde{q}}_s \right\|_2^2 = 1$$

and

$$\begin{aligned} 0 &= \tilde{q}_s^* \tilde{q}_d + \tilde{q}_d^* \tilde{q}_s \\ &= [q_{s0} q_{d0} + \vec{q}_s \cdot \vec{q}_d, -q_{d0} \vec{q}_s + q_{s0} \vec{q}_d - \vec{q}_s \times \vec{q}_d] + [q_{s0} q_{d0} + \vec{q}_s \cdot \vec{q}_d, q_{d0} \vec{q}_s - q_{s0} \vec{q}_d - \vec{q}_d \times \vec{q}_s] \\ &= \left[2(q_{s0} q_{d0} + \vec{q}_s \cdot \vec{q}_d), \vec{0} \right] \\ &= \left[2\vec{\tilde{q}}_d^\top \vec{\tilde{q}}_s, \vec{0} \right], \end{aligned}$$

which implies that $\vec{\tilde{q}}_d^\top \vec{\tilde{q}}_s = 0$. Hence, in real vector form, the unit dual quaternion set corresponds to the following set

$$\Omega := \left\{ (\vec{\tilde{q}}_s, \vec{\tilde{q}}_d) \in \mathbb{R}^8 \mid \left\| \vec{\tilde{q}}_s \right\|_2^2 = 1 \text{ and } \vec{\tilde{q}}_d^\top \vec{\tilde{q}}_s = 0 \right\}.$$

Therefore, using the real vector representation, the original projection problem (4) can be reformulated as the following non-convex optimization problem

$$(5) \quad \min_{\vec{\tilde{q}}_s, \vec{\tilde{q}}_d} f(\vec{\tilde{q}}_s, \vec{\tilde{q}}_d) := \frac{1}{2} \left\| \vec{\tilde{q}}_s - \vec{a}_s \right\|_2^2 + \frac{1}{2} \left\| \vec{\tilde{q}}_d - \vec{a}_d \right\|_2^2 \quad \text{subject to} \quad \left\| \vec{\tilde{q}}_s \right\|_2^2 = 1, \quad \vec{\tilde{q}}_d^\top \vec{\tilde{q}}_s = 0.$$

3.2. The existence of the global minimum of (5). In this subsection, we show that problem (5) admits a global minimizer. Let $\vec{\tilde{q}}_s^* = (1, 0, 0, 0)^\top$ and $\vec{\tilde{q}}_d^* = \vec{0}$. Clearly, $(\vec{\tilde{q}}_s^*, \vec{\tilde{q}}_d^*) \in \Omega$. Define

$$L_* := \left\{ (\vec{\tilde{q}}_s, \vec{\tilde{q}}_d) \mid f(\vec{\tilde{q}}_s, \vec{\tilde{q}}_d) \leq f(\vec{\tilde{q}}_s^*, \vec{\tilde{q}}_d^*) \right\}.$$

It is easy to verify that L_* is nonempty, bounded, and closed. Since Ω is closed, we conclude that $\Omega \cap L_*$ is a closed and bounded subset, and therefore compact. As the objective function $f(\vec{\tilde{q}}_s, \vec{\tilde{q}}_d)$ is continuous, the extreme value theorem guarantees that the minimum is attained on the compact set $\Omega \cap L_*$. That is, there exists $(\vec{\tilde{q}}_s^\#, \vec{\tilde{q}}_d^\#) \in \Omega \cap L_*$ such that

$$f(\vec{\tilde{q}}_s^\#, \vec{\tilde{q}}_d^\#) = \min_{(\vec{\tilde{q}}_s, \vec{\tilde{q}}_d) \in \Omega} f(\vec{\tilde{q}}_s, \vec{\tilde{q}}_d),$$

which confirms the existence of a global minimum of problem (5).

We define the constraints in problem (5) as follows:

$$c_1(\vec{\tilde{q}}_s, \vec{\tilde{q}}_d) := \left\| \vec{\tilde{q}}_s \right\|_2^2 - 1, \quad c_2(\vec{\tilde{q}}_s, \vec{\tilde{q}}_d) := \vec{\tilde{q}}_d^\top \vec{\tilde{q}}_s.$$

It is evident that the gradients $\nabla c_1(\vec{\tilde{q}}_s, \vec{\tilde{q}}_d)$ and $\nabla c_2(\vec{\tilde{q}}_s, \vec{\tilde{q}}_d)$ are linearly independent for any $(\vec{\tilde{q}}_s, \vec{\tilde{q}}_d) \in \Omega$, which implies that the LICQ holds for problem (5). By Theorem 2.3, we obtain the following proposition.

Proposition 3.1. The global minimizer $(\vec{\tilde{q}}_s^\#, \vec{\tilde{q}}_d^\#)$ of problem (5) satisfies the KKT conditions.

Our next objective is to find all feasible pairs $(\vec{\tilde{q}}_s, \vec{\tilde{q}}_d)$ that satisfy the KKT conditions associated with problem (5). Among these candidate solutions, the one that attains the smallest value of the objective function corresponds to the desired projection point.

3.3. The algorithm. In this subsection, we present our algorithm in a systematic manner. The algorithm is developed based on different cases determined by the relationship between the standard part $\vec{\tilde{a}}_s$ and the dual part $\vec{\tilde{a}}_d$. Specifically, we consider two scenarios: $\vec{\tilde{a}}_s = 0$ and $\vec{\tilde{a}}_s \neq 0$. The detailed procedure is provided in Algorithm 1.

Case 1: $\vec{\tilde{a}}_s = \vec{0}$. In this case, the constrained optimization problem (5) simplifies to

$$\min_{\vec{\tilde{q}}_s, \vec{\tilde{q}}_d} \frac{1}{2} \left\| \vec{\tilde{q}}_s \right\|_2^2 + \frac{1}{2} \left\| \vec{\tilde{q}}_d - \vec{\tilde{a}}_d \right\|_2^2 \quad \text{subject to} \quad \left\| \vec{\tilde{q}}_s \right\|_2^2 = 1, \quad \vec{\tilde{q}}_d^\top \vec{\tilde{q}}_s = 0.$$

It can be seen that the globally optimal solutions are given by $\vec{\tilde{q}}_d^\# = \vec{\tilde{a}}_d$, and any $\vec{\tilde{q}}_s^\#$ satisfying $\left\| \vec{\tilde{q}}_s^\# \right\|_2^2 = 1$ and $(\vec{\tilde{q}}_s^\#)^\top \vec{\tilde{a}}_d = 0$ is a solution to the problem. In this case, the optimal solution for $\vec{\tilde{q}}_s$ is non-unique. It lies on the intersection of the unit hypersphere and the hyperplane orthogonal to the input vector $\vec{\tilde{a}}_d$ (Figure 1, left panel).

Case 2: $\vec{\tilde{a}}_s \neq \vec{0}$. In this case, we further distinguish between two subcases: $\vec{\tilde{a}}_d = \vec{0}$ and $\vec{\tilde{a}}_d \neq \vec{0}$.

Case 2.1: $\vec{\tilde{a}}_d = \vec{0}$. In this case, the constrained optimization problem (5) becomes

$$(6) \quad \min_{\vec{\tilde{q}}_s, \vec{\tilde{q}}_d} \frac{1}{2} \left\| \vec{\tilde{q}}_s - \vec{\tilde{a}}_s \right\|_2^2 + \frac{1}{2} \left\| \vec{\tilde{q}}_d \right\|_2^2 \quad \text{subject to} \quad \left\| \vec{\tilde{q}}_s \right\|_2^2 = 1, \quad \vec{\tilde{q}}_d^\top \vec{\tilde{q}}_s = 0.$$

Note that the constraint $\left\| \vec{\tilde{q}}_s \right\|_2^2 = 1$ holds, and $\vec{\tilde{a}}_s$ is a known constant. Therefore, the objective function in (6) can be simplified to

$$(7) \quad \min_{\vec{\tilde{q}}_s, \vec{\tilde{q}}_d} - \left\langle \vec{\tilde{q}}_s, \vec{\tilde{a}}_s \right\rangle + \frac{1}{2} \left\| \vec{\tilde{q}}_d \right\|_2^2 \quad \text{subject to} \quad \left\| \vec{\tilde{q}}_s \right\|_2^2 = 1, \quad \vec{\tilde{q}}_d^\top \vec{\tilde{q}}_s = 0.$$

Case 1: $\vec{a}_s = \vec{0}$ **Case 2.1:** $\vec{a}_s \neq \vec{0}$ and $\vec{a}_d = \vec{0}$

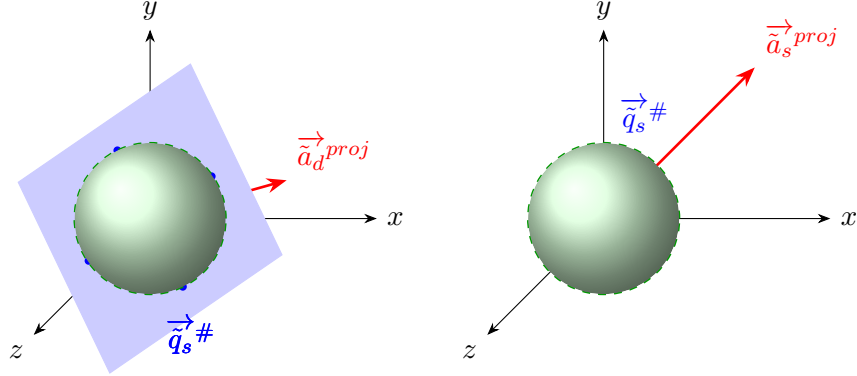


FIGURE 1. A three-dimensional geometric analogy for the vector projection problem. Left panel (**Case 1**): The non-unique solutions $\vec{q}_s^{\#}$ lie on the blue circular intersection of the green unit sphere and a plane. Right panel (**Case 2.1**): The unique solution $\vec{q}_s^{\#}$ is the radial projection of the input vector \vec{a}_s onto the green unit sphere.

It is evident that the optimal solution for \vec{q}_d is the zero vector, i.e., $\vec{q}_d^{\#} = \vec{0}$. By the Cauchy–Schwarz inequality, we have $-\langle \vec{q}_s, \vec{a}_s \rangle \geq -\|\vec{q}_s\|_2 \|\vec{a}_s\|_2$, with equality if and only if $\vec{q}_s = k\vec{a}_s$ for some constant $k \geq 0$. Since $\|\vec{q}_s\|_2 = 1$, it follows that the optimal solution for \vec{q}_s is given by $\vec{q}_s^{\#} = \frac{\vec{a}_s}{\|\vec{a}_s\|_2}$. To summarize, in this case, the unique globally optimal solution is given by

$$\vec{q}_s^{\#} = \frac{\vec{a}_s}{\|\vec{a}_s\|_2} \quad \text{and} \quad \vec{q}_d^{\#} = \vec{0}.$$

In this case, the unique solution $\vec{q}_s^{\#}$ is found by radially projecting the input vector \vec{a}_s onto the unit hypersphere (Figure 1, right panel).

Case 2.2: $\vec{a}_d \neq \vec{0}$. In this case, by Proposition 3.1, we know that the global minimizer $(\vec{q}_s^{\#}, \vec{q}_d^{\#})$ of problem (5) satisfies the KKT conditions. Our objective is to identify all feasible pairs (\vec{q}_s, \vec{q}_d) that satisfy these KKT conditions. The projection point is the one among these candidates that minimizes the objective function.

Using real multipliers λ and μ , the Lagrangian function of (5) is

$$\mathcal{L}(\vec{q}_s, \vec{q}_d, \lambda, \mu) = \frac{1}{2} \|\vec{q}_s - \vec{a}_s\|_2^2 + \frac{1}{2} \|\vec{q}_d - \vec{a}_d\|_2^2 + \lambda \left(\|\vec{q}_s\|_2^2 - 1 \right) + \mu \vec{q}_d^{\top} \vec{q}_s.$$

According to Theorem 2.3, the first-order necessary optimality conditions for (5) are given by

$$(8) \quad \vec{\tilde{q}}_s - \vec{\tilde{a}}_s + 2\lambda \vec{\tilde{q}}_s + \mu \vec{\tilde{q}}_d = \vec{0},$$

$$(9) \quad \vec{\tilde{q}}_d - \vec{\tilde{a}}_d + \mu \vec{\tilde{q}}_s = \vec{0},$$

$$(10) \quad \left\| \vec{\tilde{q}}_s \right\|_2^2 - 1 = 0,$$

$$(11) \quad \vec{\tilde{q}}_d^\top \vec{\tilde{q}}_s = 0.$$

Taking the inner product of (8) with $\vec{\tilde{q}}_s$ and using constraints (10) and (11), we obtain

$$(12) \quad \lambda = \frac{\vec{\tilde{q}}_s^\top \vec{\tilde{a}}_s - 1}{2}.$$

Similarly, taking the inner product of (9) with $\vec{\tilde{q}}_s$ yields

$$(13) \quad \mu = \vec{\tilde{q}}_s^\top \vec{\tilde{a}}_d.$$

Substituting μ back into (9), we obtain

$$\vec{\tilde{q}}_d = \vec{\tilde{a}}_d - \left(\vec{\tilde{q}}_s^\top \vec{\tilde{a}}_d \right) \vec{\tilde{q}}_s.$$

Substituting the expressions for λ , μ , and $\vec{\tilde{q}}_d$ into (8) gives

$$(14) \quad \vec{\tilde{q}}_s^\top \vec{\tilde{a}}_s \vec{\tilde{q}}_s + \vec{\tilde{q}}_s^\top \vec{\tilde{a}}_d \vec{\tilde{a}}_d - \left(\vec{\tilde{q}}_s^\top \vec{\tilde{a}}_d \right)^2 \vec{\tilde{q}}_s - \vec{\tilde{a}}_s = \vec{0}.$$

Next, we intend to take inner products of (14) with vectors $\vec{\tilde{a}}_s$ and $\vec{\tilde{a}}_d$, which lead to the following two equations

$$(15) \quad \left(\vec{\tilde{q}}_s^\top \vec{\tilde{a}}_s \right)^2 - \left(\vec{\tilde{q}}_s^\top \vec{\tilde{a}}_d \right)^2 \left(\vec{\tilde{q}}_s^\top \vec{\tilde{a}}_s \right) + \left(\vec{\tilde{q}}_s^\top \vec{\tilde{a}}_d \right) \left(\vec{\tilde{a}}_d^\top \vec{\tilde{a}}_s \right) - \left\| \vec{\tilde{a}}_s \right\|_2^2 = 0$$

and

$$(16) \quad \left(\vec{\tilde{q}}_s^\top \vec{\tilde{a}}_s \right) \left(\vec{\tilde{q}}_s^\top \vec{\tilde{a}}_d \right) + \left(\vec{\tilde{q}}_s^\top \vec{\tilde{a}}_d \right) \left\| \vec{\tilde{a}}_d \right\|_2^2 - \left(\vec{\tilde{q}}_s^\top \vec{\tilde{a}}_d \right)^3 - \vec{\tilde{a}}_s^\top \vec{\tilde{a}}_d = 0.$$

Note that when vectors $\vec{\tilde{a}}_s$ and $\vec{\tilde{a}}_d$ are linearly dependent, (15) and (16) become equivalent and hence reduce to a single equation, which could simplify the problem. Therefore, we further distinguish between the following two subcases: $\left\langle \vec{\tilde{a}}_s, \vec{\tilde{a}}_d \right\rangle^2 = \left\| \vec{\tilde{a}}_s \right\|_2^2 \left\| \vec{\tilde{a}}_d \right\|_2^2$ and $\left\langle \vec{\tilde{a}}_s, \vec{\tilde{a}}_d \right\rangle^2 \neq \left\| \vec{\tilde{a}}_s \right\|_2^2 \left\| \vec{\tilde{a}}_d \right\|_2^2$.

Case 2.2.1: $\left\langle \vec{\tilde{a}}_s, \vec{\tilde{a}}_d \right\rangle^2 = \left\| \vec{\tilde{a}}_s \right\|_2^2 \left\| \vec{\tilde{a}}_d \right\|_2^2$. Since $\vec{\tilde{a}}_s \neq \vec{0}$ and $\vec{\tilde{a}}_d \neq \vec{0}$, this equality implies that $\vec{\tilde{a}}_s = k \vec{\tilde{a}}_d$ for some scalar $k \neq 0$. Substituting (13) and $\vec{\tilde{a}}_s = k \vec{\tilde{a}}_d$ into (16), we obtain

the following univariate cubic equation in μ

$$(17) \quad -\mu^3 + k\mu^2 + \left\| \vec{\tilde{a}}_d \right\|_2^2 \mu - k \left\| \vec{\tilde{a}}_d \right\|_2^2 = 0,$$

whose three roots are explicitly given by

$$\mu_1 = k, \mu_2 = \left\| \vec{\tilde{a}}_d \right\|_2, \text{ and } \mu_3 = -\left\| \vec{\tilde{a}}_d \right\|_2.$$

If $\mu = k$, then by equation (9) we have

$$\vec{\tilde{q}}_s = \frac{\vec{\tilde{a}}_d - \vec{\tilde{q}}_d}{k}.$$

Substituting this expression and $\vec{\tilde{a}}_s = k\vec{\tilde{a}}_d$ into (5), the original optimization problem reduces to

$$\min_{\vec{\tilde{q}}_d} \frac{1}{2} \left\| \vec{\tilde{q}}_d \right\|_2^2 + C_1 \quad \text{subject to} \quad \vec{\tilde{q}}_d^\top \vec{\tilde{q}}_s = 0, \quad \left\| \vec{\tilde{q}}_s \right\|_2^2 = 1,$$

where $C_1 = \frac{1}{2} + \frac{k^2-1}{2} \left\| \vec{\tilde{a}}_d \right\|_2^2$ is a constant independent of $\vec{\tilde{q}}_d$ and $\vec{\tilde{q}}_s$. The minimum is attained when $\vec{\tilde{q}}_d = \vec{0}$, which implies $\vec{\tilde{q}}_s = \frac{\vec{\tilde{a}}_d}{k}$. Therefore, for the case where $\mu = k$, the minimizers are given by

$$\vec{\tilde{q}}_d^\# = \vec{0}, \quad \vec{\tilde{q}}_s^\# = \frac{\vec{\tilde{a}}_d}{k}.$$

Now consider the case where $\mu \neq k$, i.e., $\mu = \left\| \vec{\tilde{a}}_d \right\|_2 \neq k$ or $\mu = -\left\| \vec{\tilde{a}}_d \right\|_2 \neq k$. Since $\vec{\tilde{a}}_s = k\vec{\tilde{a}}_d$, it follows from (13) and (12) that

$$\lambda = \frac{k\mu - 1}{2}.$$

Substituting this expression into the optimality conditions (8) and (9), we get

$$(18) \quad \mu(k - \mu)\vec{\tilde{q}}_s = (k - \mu)\vec{\tilde{a}}_d, \quad \text{and} \quad (k - \mu)\vec{\tilde{q}}_d = \vec{0}.$$

Since $\mu \neq k$, we conclude that

$$\vec{\tilde{q}}_d^\# = \vec{0}, \quad \vec{\tilde{q}}_s^\# = \frac{\vec{\tilde{a}}_d}{\mu}.$$

To summarize, regardless of whether $\mu = k$ or $\mu \neq k$, the optimal solution takes the form

$$\vec{\tilde{q}}_d^\# = \vec{0}, \quad \vec{\tilde{q}}_s^\# = \frac{\vec{\tilde{a}}_d}{\mu}.$$

Substituting this solution into the objective function in (5) yields

$$\left(\frac{1}{\mu^2} - 2 \frac{k}{\mu} \right) \left\| \vec{\tilde{a}}_d \right\|_2^2 + C_2,$$

where $C_2 = (\frac{1}{2} + k^2) \left\| \vec{\tilde{a}}_d \right\|_2^2$ is a constant. The optimal μ is then obtained by minimizing the scalar expression

$$\mu^* \in \operatorname{argmin}_{\mu \in \{k, \left\| \vec{\tilde{a}}_d \right\|_2, -\left\| \vec{\tilde{a}}_d \right\|_2\}} \left\{ \frac{1}{\mu^2} - 2 \frac{k}{\mu} \right\}.$$

Hence, for the case where $\left\langle \vec{\tilde{a}}_s, \vec{\tilde{a}}_d \right\rangle^2 = \left\| \vec{\tilde{a}}_s \right\|_2^2 \left\| \vec{\tilde{a}}_d \right\|_2^2$, the complete procedure for determining the optimal solution $(\vec{\tilde{q}}_s^\#, \vec{\tilde{q}}_d^\#)$ is formally summarized in Stage I.

Stage I

1: Compute

$$\mu^* \in \operatorname{argmin}_{\mu \in \{k, \left\| \vec{\tilde{a}}_d \right\|_2, -\left\| \vec{\tilde{a}}_d \right\|_2\}} \left\{ \frac{1}{\mu^2} - 2 \frac{k}{\mu} \right\}.$$

2: Set $\vec{\tilde{q}}_d^\# = \vec{0}$ and $\vec{\tilde{q}}_s^\# = \frac{\vec{\tilde{a}}_d}{\mu^*}$.

Case 2.2.2: $\left\langle \vec{\tilde{a}}_s, \vec{\tilde{a}}_d \right\rangle^2 \neq \left\| \vec{\tilde{a}}_s \right\|_2^2 \left\| \vec{\tilde{a}}_d \right\|_2^2$. In this case, the strict inequality implies that $\vec{\tilde{a}}_s$ and $\vec{\tilde{a}}_d$ are linearly independent. A related analysis for this case has also been discussed in [2]. From (12) and (13), we have

$$\vec{\tilde{q}}_s^\# \top \vec{\tilde{a}}_s = 2\lambda + 1 \text{ and } \vec{\tilde{q}}_s^\# \top \vec{\tilde{a}}_d = \mu.$$

Substituting these expressions into (15) and (16), we obtain the following coupled equations in (λ, μ)

$$(19) \quad (2\lambda + 1)^2 - (2\lambda + 1)\mu^2 + \mu \vec{\tilde{a}}_s^\# \top \vec{\tilde{a}}_d - \left\| \vec{\tilde{a}}_s \right\|_2^2 = 0,$$

$$(20) \quad (2\lambda + 1)\mu + \mu \left\| \vec{\tilde{a}}_d \right\|_2^2 - \mu^3 - \vec{\tilde{a}}_s^\# \top \vec{\tilde{a}}_d = 0.$$

From (20), we can isolate the term $(2\lambda + 1)\mu$ as

$$(2\lambda + 1)\mu = -\mu \left\| \vec{\tilde{a}}_d \right\|_2^2 + \mu^3 + \vec{\tilde{a}}_s^\# \top \vec{\tilde{a}}_d.$$

Multiplying equation (19) by μ^2 and substituting the above identity into it, we eliminate λ and obtain the following quartic polynomial in μ ,

$$(21) \quad -\left\| \vec{\tilde{a}}_d \right\|_2^2 \mu^4 + 2 \vec{\tilde{a}}_s^\# \top \vec{\tilde{a}}_d \mu^3 + \left(\left\| \vec{\tilde{a}}_d \right\|_2^4 - \left\| \vec{\tilde{a}}_s \right\|_2^2 \right) \mu^2 - 2 \vec{\tilde{a}}_s^\# \top \vec{\tilde{a}}_d \left\| \vec{\tilde{a}}_d \right\|_2^2 \mu + (\vec{\tilde{a}}_s^\# \top \vec{\tilde{a}}_d)^2 = 0.$$

All real roots μ of the quartic equation (21) can be found numerically using a standard polynomial root solver, e.g., in MATLAB. Once a real root μ is identified, the corresponding value of λ is obtained using equation (19) if $\mu = 0$, or equation (20) if $\mu \neq 0$.

Subsequently, from the optimality conditions (8) and (9), the pair $(\vec{\tilde{q}}_s, \vec{\tilde{q}}_d)$ can be recovered explicitly as

$$(22) \quad \vec{\tilde{q}}_s = \frac{\vec{\tilde{a}}_s - \mu \vec{\tilde{a}}_d}{2\lambda - \mu^2 + 1} \quad \text{and} \quad \vec{\tilde{q}}_d = \frac{-\mu \vec{\tilde{a}}_s + (2\lambda + 1) \vec{\tilde{a}}_d}{2\lambda - \mu^2 + 1}.$$

Therefore, for each real root μ , we compute the associated (λ, μ) and then obtain candidate solutions $(\vec{\tilde{q}}_s, \vec{\tilde{q}}_d)$ via (22). Among all such candidates, we select the one that yields the minimum value of the original objective function in (5). In particular, when $\mu = 0$, equation (19) reduces to $(2\lambda + 1)^2 = \|\vec{\tilde{a}}_s\|_2^2$, and hence the corresponding values of λ are $\lambda = \frac{-1 \pm \|\vec{\tilde{a}}_s\|_2}{2}$. The two candidates lead to objective function values $(1 - \|\vec{\tilde{a}}_s\|_2)^2$ and $(1 + \|\vec{\tilde{a}}_s\|_2)^2$, respectively. Since $(1 - \|\vec{\tilde{a}}_s\|_2)^2 < (1 + \|\vec{\tilde{a}}_s\|_2)^2$ for all $\|\vec{\tilde{a}}_s\|_2 > 0$, the value $\lambda = \frac{-1 + \|\vec{\tilde{a}}_s\|_2}{2}$ yields the smaller objective value and is therefore selected.

Hence, for the case where $\langle \vec{\tilde{a}}_s, \vec{\tilde{a}}_d \rangle^2 \neq \|\vec{\tilde{a}}_s\|_2^2 \|\vec{\tilde{a}}_d\|_2^2$, the complete procedure for determining the optimal solution $(\vec{\tilde{q}}_s^\#, \vec{\tilde{q}}_d^\#)$ is formally summarized in Stage II.

Stage II

```

1: Solve equation (21) and extract all real roots  $\mu^{(1)}, \dots, \mu^{(\ell)}$ , where  $1 \leq \ell \leq 4$ .
2: for  $i = 1, \dots, \ell$  do
3:   if  $\mu^{(i)} = 0$  then
4:     Set  $\vec{\tilde{q}}_s^{(i)} = \frac{\vec{\tilde{a}}_s}{\|\vec{\tilde{a}}_s\|_2}$ ,  $\vec{\tilde{q}}_d^{(i)} = \vec{\tilde{a}}_d$ , and  $f^{(i)} = (1 - \|\vec{\tilde{a}}_s\|_2)^2$ .
5:   else
6:     Compute  $\lambda^{(i)}$  by solving equation (20). Evaluate  $\vec{\tilde{q}}_s^{(i)}$  and  $\vec{\tilde{q}}_d^{(i)}$  using (22). Then compute the objective function value
7:     
$$f^{(i)} = \frac{1}{2} \left\| \vec{\tilde{q}}_s^{(i)} - \vec{\tilde{a}}_s \right\|_2^2 + \frac{1}{2} \left\| \vec{\tilde{q}}_d^{(i)} - \vec{\tilde{a}}_d \right\|_2^2.$$

8:   end if
9: end for
9: Set  $\vec{\tilde{q}}_s^\# = \vec{\tilde{q}}_s^{(i^*)}$ ,  $\vec{\tilde{q}}_d^\# = \vec{\tilde{q}}_d^{(i^*)}$ , where  $i^* \in \arg \min_{i \in \{1, \dots, \ell\}} f^{(i)}$ .

```

The above analysis leads to the following unified procedure for projecting a general dual quaternion onto the unit dual quaternion set, as summarized in Algorithm 1.

Algorithm 1 Projection onto the unit dual quaternion set.

```

1: Input: General dual quaternion  $\hat{a} = \tilde{a}_s + \tilde{a}_d\epsilon$  and transform into vectors  $\vec{\tilde{a}}_s$  and  $\vec{\tilde{a}}_d$ .
2: Output: Projected vectors  $\vec{\tilde{q}}_s^\#$ ,  $\vec{\tilde{q}}_d^\#$  such that  $\hat{q} = \tilde{q}_s^\# + \tilde{q}_d^\#\epsilon$  is a unit dual quaternion.
3: if  $\vec{\tilde{a}}_s = \vec{0}$  then
4:     Set  $\vec{\tilde{q}}_d^\# = \vec{\tilde{a}}_d$  then find  $\vec{\tilde{q}}_s^\#$  satisfying  $(\vec{\tilde{q}}_s^\#)^\top \vec{\tilde{a}}_d = 0$  and  $\left\| \vec{\tilde{q}}_s^\# \right\|_2^2 = 1$ .
5: else
6:     if  $\vec{\tilde{a}}_d = \vec{0}$  then
7:         Set  $\vec{\tilde{q}}_s^\# = \frac{\vec{\tilde{a}}_s}{\left\| \vec{\tilde{a}}_s \right\|_2}$  and  $\vec{\tilde{q}}_d^\# = \vec{0}$ .
8:     else
9:         if  $\langle \vec{\tilde{a}}_s, \vec{\tilde{a}}_d \rangle^2 = \left\| \vec{\tilde{a}}_s \right\|_2^2 \left\| \vec{\tilde{a}}_d \right\|_2^2$  then
10:            Set  $\vec{\tilde{q}}_s^\#$  and  $\vec{\tilde{q}}_d^\#$  by Stage I.
11:        else
12:            Set  $\vec{\tilde{q}}_s^\#$  and  $\vec{\tilde{q}}_d^\#$  by Stage II.
13:        end if
14:    end if
15: end if
16: Projected unit dual quaternion  $\hat{q} = \tilde{q}_s^\# + \tilde{q}_d^\#\epsilon$ .

```

4. NUMERICAL EXAMPLES

In this section, we conduct numerical experiments to evaluate the numerical performance of the unit dual quaternion projection algorithm (Algorithm 1) proposed in this paper. All the experiments are implemented in MATLAB for Windows 11 on a LAPTOP PC with an Intel Core Ultra 7 155H @ 1.40 GHz and 32 GB memory. All experimental results were obtained using double-precision floating-point format.

4.1. Synthetic data. First of all, we verify that the Algorithm 1 can accurately project general dual quaternions onto the unit dual quaternion set with high precision using simulated data. To this end, we apply the following procedure:

- 1) For given n and $\kappa > 1$, we construct a dense matrix $\mathbf{A}_s = [\vec{\tilde{a}}_{s_1}, \vec{\tilde{a}}_{s_2}, \dots, \vec{\tilde{a}}_{s_n}]$ by $\mathbf{A}_s = \mathbf{UDV}^\top$, where $\mathbf{U} \in \mathbb{R}^{4 \times r}$, $\mathbf{D} \in \mathbb{R}^{r \times r}$, and $\mathbf{V} \in \mathbb{R}^{n \times r}$. Using MATLAB syntax, these matrices are generated by $[\mathbf{U}, \sim] = \text{qr}(\text{randn}(4, r), 0)$, $[\mathbf{V}, \sim] = \text{qr}(\text{randn}(n, r), 0)$, and $\mathbf{D} = \text{diag}(1 + (\kappa - 1) \cdot \text{rand}(r, 1))$. Subsequently, we randomly select 10% of the column vectors $\vec{\tilde{a}}_{s_i}$ and set them to zero.

2) Randomly generate vectors $\mathbf{t}_i (i = 1, \dots, n)$ representing translation in 3D space. They are uniform distribution within the euclidean cube $[-5, 5]^3$ in \mathbb{R}^3 . Then convert them to pure quaternions in real vector that form the dual parts $\tilde{\vec{a}}_{d_i}$ of dual quaternions. The $\{\tilde{\vec{a}}_{d_i}\}$ are concatenated into matrix $\mathbf{A}_d = [\tilde{\vec{a}}_{d_1}, \tilde{\vec{a}}_{d_2}, \dots, \tilde{\vec{a}}_{d_n}] \in \mathbb{R}^{4 \times n}$. Similarly, we randomly set 10% of the column vectors $\tilde{\vec{a}}_{d_i}$ to zero.

3) Taking $(\tilde{\vec{a}}_{s_i}, \tilde{\vec{a}}_{d_i})$ as inputs, substituting them into Algorithm 1 to obtain outputs $(\tilde{\vec{q}}_{s_i}, \tilde{\vec{q}}_{d_i})$, and compute:

- 1) The rotation error, $E_R = \left| \left\| \tilde{\vec{q}}_{s_i} \right\|_2^2 - 1 \right|$, measuring the unitarity of the standard part of the unit dual quaternions.
- 2) The orthogonality error, $E_O = \left| \tilde{\vec{q}}_{s_i}^\top \tilde{\vec{q}}_{d_i} \right|$, quantifying the orthogonality between the dual part and the standard part of the unit dual quaternions.

4) Draw the cumulative distribution function (CDF) plots of norm error and orthogonal error.

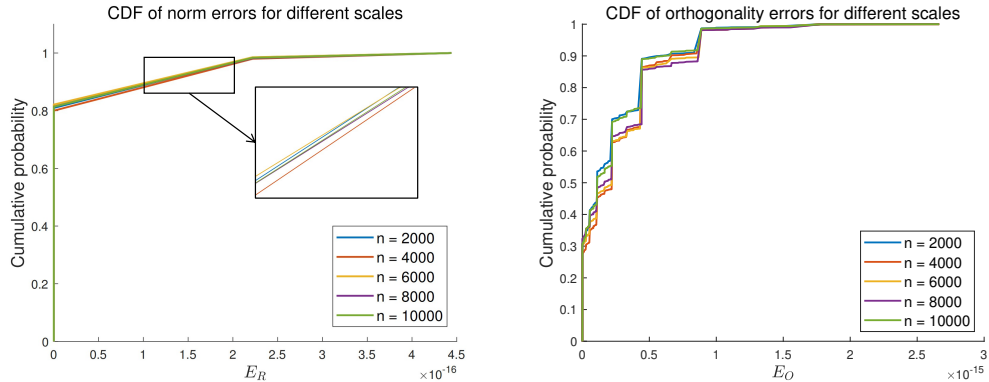


FIGURE 2. Figures depict the cumulative distribution of norm errors (E_R) and orthogonality errors (E_O) across increasing problem dimensions.

In Fig.2, we plot the cumulative distribution of norm errors E_R (left panel) and orthogonality errors E_O (right panel), where $n = 2000, 4000, \dots, 10000$ and $\kappa = 10$. Table 1 summarizes the statistical comparison between our method and the projection method (PM) proposed in [6] on the synthetic datasets. While both methods demonstrate high precision in satisfying the unit norm and orthogonality constraints, with errors at the level of machine precision, a crucial distinction emerges when evaluating the primary optimization objective: the compactness of the solution in the 2^R norm distance metric in (4).

TABLE 1. Error statistics and 2^R norm distance comparison for our method and the PM method proposed in [6].

n	Method	E_R	E_O	2^R Norm Distance
2000	Ours	3.8747×10^{-17}	2.3772×10^{-16}	1.1408×10^0
	PM	5.8842×10^{-18}	3.7983×10^{-15}	2.9966×10^1
4000	Ours	3.7692×10^{-17}	2.3448×10^{-16}	1.0989×10^0
	PM	6.6058×10^{-18}	5.7301×10^{-15}	4.3934×10^1
6000	Ours	3.9524×10^{-17}	2.2959×10^{-16}	1.0758×10^0
	PM	8.8448×10^{-18}	7.9683×10^{-15}	7.2922×10^1
8000	Ours	3.9191×10^{-17}	2.3094×10^{-16}	1.0899×10^0
	PM	6.8834×10^{-18}	6.3036×10^{-15}	5.2992×10^1
10000	Ours	3.8414×10^{-17}	2.0436×10^{-16}	1.0631×10^0
	PM	5.1514×10^{-18}	8.9374×10^{-15}	6.9591×10^1

The core advantage of our algorithm is highlighted by the mean 2^R norm distance, which measures how close the projection is to the original point. Our method consistently produces an optimal projection, with a mean 2^R norm distance stable at approximately 1.1. In stark contrast, the solution from the power method yields a mean 2^R norm distance that is orders of magnitude larger, ranging from 30 to over 70 times greater than ours, and this distance increases with the problem size. This significant difference indicates that while the power method can find a point that satisfies the algebraic constraints, it is not the closest point on the unit dual quaternion manifold. The method fails to find the optimal solution with respect to the 2^R norm distance.

4.2. Real-world data. In this section, we employ real-world datasets “Dataset 1” from [16], “Dataset 2” from [9] for testing Algorithm 1. Each dataset comprises multiple sets of poses exhibiting inherent noise characteristics. For the real-world data experiments, we first separate the data into its standard (\mathbf{A}_s) and dual (\mathbf{A}_d) parts as input to Algorithm 1. Tables 2 and 3 report the performance of our method and the projection method proposed in [6] on the “Dataset 1” and “Dataset 2” benchmarks, respectively.

Across both sets of experiments, both methods demonstrate excellent precision in satisfying the unit norm constraint, with the mean E_R consistently at the level of machine precision. However, a notable difference emerges in the E_O . While our method maintains

this error at a stable, high precision (typically 10^{-16} or better), the power method exhibits instability on several datasets. Most importantly, the results for the mean 2^R norm distance confirm the superior optimality of our approach. Across nearly all datasets, our method achieves a smaller distance value.

TABLE 2. Comparison of our method and the PM method proposed in [6] on “Dataset 1”.

Dataset	Scale	Method	E_R	E_O	2^R Norm Distance
FB1 XYZ	2335	Ours	7.6161×10^{-17}	7.1498×10^{-17}	8.4100×10^{-2}
		PM	1.3693×10^{-17}	8.6338×10^{-17}	1.9190×10^{-1}
FB1 Desk	3000	Ours	7.3888×10^{-17}	4.6513×10^{-17}	1.4150×10^{-1}
		PM	6.7517×10^{-18}	8.0664×10^{-17}	2.7780×10^{-1}
FB1 360	2870	Ours	7.2958×10^{-17}	2.7259×10^{-17}	4.2160×10^{-1}
		PM	8.9746×10^{-18}	1.5441×10^{-16}	7.2900×10^{-1}
FB1 Floor	4427	Ours	7.2427×10^{-17}	3.2843×10^{-17}	4.1240×10^{-1}
		PM	9.1286×10^{-18}	1.0890×10^{-16}	5.2400×10^{-1}
FB1 Room	4887	Ours	7.0653×10^{-17}	3.9797×10^{-17}	3.4470×10^{-1}
		PM	7.3606×10^{-18}	1.5385×10^{-16}	6.8440×10^{-1}
FB2 LNL	6476	Ours	6.8780×10^{-17}	7.9341×10^{-17}	4.3130×10^{-1}
		PM	7.7832×10^{-18}	2.5900×10^{-16}	1.1316×10^0
FB2 LWL	12284	Ours	6.2850×10^{-17}	7.3724×10^{-17}	6.7160×10^{-1}
		PM	9.7791×10^{-18}	2.7185×10^{-16}	1.2298×10^0
FB2 XYZ	20975	Ours	6.9599×10^{-17}	2.2466×10^{-17}	4.5530×10^{-1}
		PM	1.7887×10^{-17}	2.0445×10^{-16}	9.3540×10^{-1}
FB2 Desk	36820	Ours	7.0257×10^{-17}	6.2599×10^{-17}	3.6470×10^{-1}
		PM	8.3702×10^{-18}	9.0848×10^{-05}	9.8560×10^{-1}
FB3 NNF	1580	Ours	5.7900×10^{-17}	6.5595×10^{-17}	5.3830×10^{-1}
		PM	0.0000×10^0	2.8261×10^{-16}	1.3698×10^0
FB3 NNN	3772	Ours	6.2457×10^{-17}	5.5881×10^{-17}	7.0290×10^{-1}
		PM	6.8285×10^{-18}	3.2717×10^{-16}	1.5472×10^0
FB3 LO	8710	Ours	7.0106×10^{-17}	6.5510×10^{-17}	4.5090×10^{-1}
		PM	7.6734×10^{-18}	1.3637×10^{-3}	1.0069×10^0

TABLE 3. Comparison of our method and the PM method proposed in [6] on “Dataset 2”.

Dataset	Scale	Method	Mean E_R	Mean E_O	Mean 2^R Norm	Distance
FC1 IO	98	Ours	7.0239×10^{-17}	1.6905×10^{-18}	1.5518×10^{-1}	
		PM	9.0630×10^{-18}	3.1464×10^{-17}	1.6195×10^{-1}	
FC1 Vicon	72	Ours	8.0183×10^{-17}	3.3923×10^{-17}	3.1193×10^{-1}	
		PM	3.0840×10^{-18}	9.2844×10^{-17}	4.8741×10^{-1}	
FC3 IO1	460	Ours	7.9646×10^{-17}	9.0694×10^{-18}	7.9962×10^{-2}	
		PM	3.8616×10^{-18}	2.4696×10^{-17}	1.2199×10^{-1}	
FC3 IO2	949	Ours	8.3296×10^{-17}	1.9667×10^{-17}	1.0601×10^{-1}	
		PM	4.4456×10^{-18}	1.4601×10^{-16}	7.1098×10^{-1}	
FC3 Vicon	951	Ours	6.5609×10^{-17}	3.9827×10^{-17}	4.8571×10^{-1}	
		PM	6.5376×10^{-18}	1.4877×10^{-16}	6.8453×10^{-1}	
FC4 IO	1689	Ours	5.7187×10^{-17}	1.8811×10^{-17}	1.5863×10^0	
		PM	3.9440×10^{-18}	1.4176×10^{-4}	1.6883×10^0	
FC4 Vicon	1640	Ours	4.3597×10^{-17}	3.3169×10^{-17}	8.4234×10^{-1}	
		PM	5.2803×10^{-18}	1.2974×10^{-16}	8.6619×10^{-1}	
Falcon5 IO	1779	Ours	5.2172×10^{-17}	2.3440×10^{-17}	1.3876×10^0	
		PM	5.8663×10^{-18}	3.3610×10^{-17}	1.4531×10^0	
Falcon5 Vicon	1336	Ours	3.9223×10^{-17}	3.2479×10^{-17}	8.1660×10^{-1}	
		PM	5.1522×10^{-18}	1.2459×10^{-16}	8.4589×10^{-1}	

5. CONCLUSION

This paper presents a systematical study on the projection problem for unit dual quaternions, offering a novel algorithm that generalizes existing methods (see Algorithm 1). By formulating the problem using the real representation of dual quaternions, we map each dual quaternion to two 4-dimensional real vectors. The numerical examples demonstrate the algorithm’s superiority. Not only does it achieve machine-level precision in satisfying the unit norm and orthogonality constraints, but more importantly, it exhibits clear optimality in the 2^R -norm distance metric when compared to other projection method.

The results contribute to the research on dual quaternion, particularly in fields such as robotics, hand-eye calibration, and rigid body motion representation. Future work could

explore further optimizations of the algorithm and its applications in more complex robotic systems.

REFERENCES

- [1] G. Brambley and J. Kim. Unit dual quaternion-based pose optimisation for visual runway observations. *IET Cyber-Systems and Robotics*, 2(4):181–189, 2020.
- [2] L. Can, Y. Chen, and D. Li. A proximal linearized algorithm for dual quaternion optimization with applications in hand-eye calibration. *Pacific Journal of Optimization*, 2023.
- [3] Z. Chen, C. Ling, L. Qi, and H. Yan. A regularization-patching dual quaternion optimization method for solving the hand-eye calibration problem. *J. Optim. Theory Appl.*, 200(3):1193–1215, Jan. 2024.
- [4] J. Cheng, J. Kim, Z. Jiang, and W. Che. Dual quaternion-based graphical slam. *Robotics and Autonomous Systems*, 77:15–24, 2016.
- [5] W. K. Clifford. Preliminary sketch of biquaternions. *Proceedings of The London Mathematical Society*, pages 381–395, 1871.
- [6] C. Cui and L. Qi. A power method for computing the dominant eigenvalue of a dual quaternion hermitian matrix. *Journal of Scientific Computing*, 100(1):21, 2024.
- [7] K. Daniilidis. Hand-eye calibration using dual quaternions. *The International Journal of Robotics Research*, 18(3):286–298, 1999.
- [8] K. Daniilidis and E. Bayro-Corrochano. The dual quaternion approach to hand-eye calibration. In *Proceedings of 13th International Conference on Pattern Recognition*, volume 1, pages 318–322. IEEE, 1996.
- [9] F. Furrer, M. Fehr, T. Novkovic, H. Sommer, I. Gilitschenski, and R. Siegwart. *Evaluation of Combined Time-Offset Estimation and Hand-Eye Calibration on Robotic Datasets*. Springer International Publishing, Cham, 2017.
- [10] J. I. Giribet, H. N. Marciano, I. Mas, A. S. Ghersin, D. K. D. Villa, and M. Sarcinelli-Filho. Dual quaternion-based control for dynamic robot formations. In *2025 International Conference on Unmanned Aircraft Systems (ICUAS)*, pages 526–533. IEEE, 2025.
- [11] D.-P. Han, Q. Wei, and Z.-X. Li. Kinematic control of free rigid bodies using dual quaternions. *International Journal of Automation and Computing*, 5(3):319–324, 2008.

- [12] C. Ling, C. Pan, and L. Qi. A metric function for dual quaternion matrices and related least-squares problems. *Linear and Multilinear Algebra*, pages 1–24, 2025.
- [13] J. Nocedal and S. J. Wright. *Numerical optimization*. Springer, 2006.
- [14] L. Qi. Standard dual quaternion optimization and its applications in hand-eye calibration and slam. *Communications on Applied Mathematics and Computation*, 5(4):1469–1483, 2023.
- [15] L. Qi, C. Ling, and H. Yan. Dual quaternions and dual quaternion vectors. *Communications on Applied Mathematics and Computation*, 4(4):1494–1508, 2022.
- [16] J. Sturm, N. Engelhard, F. Endres, W. Burgard, and D. Cremers. A benchmark for the evaluation of rgb-d slam systems. In *2012 IEEE/RSJ international conference on intelligent robots and systems*, pages 573–580. IEEE, 2012.
- [17] R. Tao, Y. Li, M. Zhang, X. Liu, and M. Wei. Solving the qly least squares problem of dual quaternion matrix equation based on stp of dual quaternion matrices. *Symmetry*, 16(9):1117, 2024.
- [18] J. Vince. *Rotation transforms for computer graphics*. Springer Science & Business Media, 2011.
- [19] H. Wang, C. Cui, and Y. Wei. The qly least-squares and the qly least-squares minimal-norm of linear dual least squares problems. *Linear and Multilinear Algebra*, 72(12):1985–2002, 2024.
- [20] P. Wang and T. Wang. Dynamic modeling and control of multibody systems using dual quaternions. *Journal of Guidance, Control, and Dynamics*, 47(8):1737–1747, 2024.
- [21] X. Wang, C. Yu, and Z. Lin. A dual quaternion solution to attitude and position control for rigid-body coordination. *IEEE Transactions on Robotics*, 28(5):1162–1170, 2012.
- [22] H. Zhu and M. K. Ng. The subspace constrained least squares solution of unit dual quaternion vector equations and its application to hand-eye calibration. *Journal of Scientific Computing*, 103(2):49, 2025.

SCHOOL OF MATHEMATICAL SCIENCES, BEIHANG UNIVERSITY, BEIJING, 100191, CHINA.

Email address: lzyang0114@buaa.edu.cn

LMIB OF THE MINISTRY OF EDUCATION, SCHOOL OF MATHEMATICAL SCIENCES, BEIHANG UNIVERSITY, BEIJING, 100191, CHINA.

Email address: chunfengcui@buaa.edu.cn

LMIB OF THE MINISTRY OF EDUCATION, SCHOOL OF MATHEMATICAL SCIENCES, BEIHANG UNIVERSITY, BEIJING, 100191, CHINA.

Email address: xiejx@buaa.edu.cn